Structural and magnetic properties of η-phase manganese nitride films grown by molecular-beam epitaxy

Haiqiang Yang, Hamad Al-Brithen, and Arthur R. Smith[a)]
Department of Physics and Astronomy, Ohio University, Athens, Ohio 45701

J. A. Borchers, R. L. Cappelletti, and M. D. Vaudin
National Institute of Standards and Technology, Gaithersburg, Maryland 208990-8562

(Received 20 March 2001; accepted for publication 20 April 2001)

Face-centered tetragonal (fct) η-phase manganese nitride films have been grown on magnesium oxide (001) substrates by molecular-beam epitaxy. For growth conditions described here, reflection high energy electron diffraction and neutron scattering show primarily two types of domains rotated by 90° to each other with their *c* axes in the surface plane. Scanning tunneling microscopy images reveal surface domains consisting of row structures which correspond directly to the bulk domains. Neutron diffraction data confirm that the Mn moments are aligned in a layered antiferromagnetic structure. The data are consistent with the fct model of G. Kreiner and H. Jacobs for bulk Mn_3N_2 [J. Alloys Compd. **183**, 345 (1992)]. © *2001 American Institute of Physics.*
[DOI: 10.1063/1.1378800]

Transition metal (TM) nitride materials, such as ScN and TiN, have amazing structural and electronic properties.[1–7] Various TM nitrides, including CoN, FeN, and MnN,[8–11] are also promising as magnetic materials with the potential for unique applications in magnetic recording and sensing. Even more fascinating is the possibility that a magnetic nitride material might be combined with the GaN system to form *nitride spintronics*. Indeed, it has been predicted that a MnGaN alloy might have a Curie temperature higher than 300 K,[12] which could make room-temperature spintronic devices possible.[13,14] It is thus of great interest to investigate the growth and properties of magnetic nitrides, in general, and manganese nitride, in particular.

Manganese nitride (Mn–N) is known to form different bulk phases, including θ (MnN), η (Mn_3N_2), ϵ (Mn_4N), and ζ (Mn_5N_2, Mn_2N, and $Mn_2N_{0.86}$).[8,9] Yet, nothing is known regarding the thin film growth of Mn–N, which is important for device applications. Therefore, we have recently used molecular beam epitaxy (MBE) to investigate the growth of Mn–N. In this letter, we report the growth of smooth, epitaxial layers of Mn–N on MgO(001) substrates using rf MBE. We have found that the η phase (Mn_3N_2) is commonly obtained for a range of growth conditions. Here, we focus on the detailed crystal and magnetic structure of the film, showing that it has the layered antiferromagnetic fct structure described by Kreiner and Jacobs for bulk Mn_3N_2,[8] and with the *c* axis in the growth plane. We also show by scanning tunneling microscopy (STM) images that a unique surface structure corresponds to the bulk structure of the film.

The experiments are performed in a custom-designed ultrahigh vacuum system consisting of a MBE chamber coupled to a surface analysis chamber. After being heated up to 1000 °C for 30 min with the nitrogen plasma on, the MgO substrate temperature is lowered to 450 °C prior to the growth of Mn–N. The nitrogen flow rate is about 1.1 sccm (growth chamber pressure is 1.1×10^{-5} Torr) with the rf power set at 500 W. The Mn flux is about $3.5\times10^{14}/cm^2s$. The growth condition is monitored using reflection high energy electron diffraction (RHEED). Following growth, the samples are investigated with *in situ* STM. After removal from the analysis chamber, the samples are analyzed using neutron scattering (NS).

The RHEED patterns shown in Fig. 1 present the stages of the growth process. After heating, the MgO(001) surface

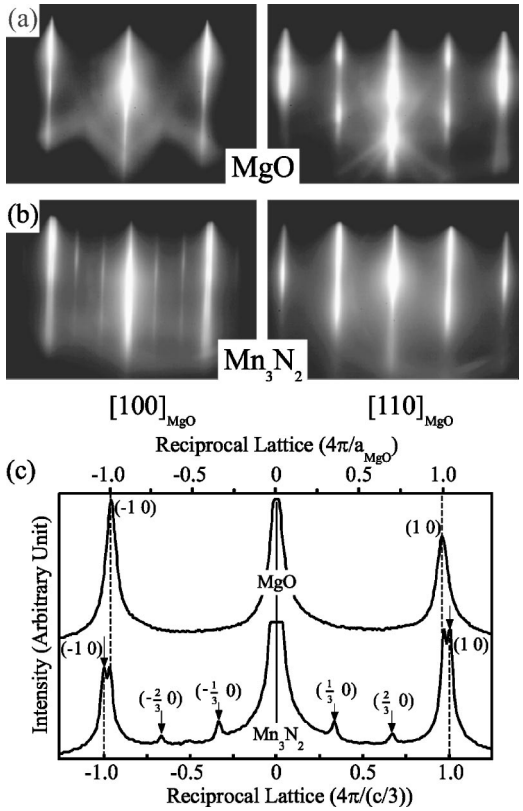

FIG. 1. RHEED patterns and line profiles of MgO and η Mn_3N_2 are shown. (a) MgO surface after 30 min of heating at 1000 °C and cooling down to 450 °C; (b) η Mn_3N_2 surface obtained following growth near 25 °C, left-hand side panel along $[100]_{MgO}$ and right panel along $[110]_{MgO}$. (c) Line profiles of MgO (top) and η Mn_3N_2 (bottom) along $[100]_{MgO}$.

a)Author to whom all correspondence should be addressed; electronic mail: smitha2@ohio.edu

exhibits streaky RHEED patterns at 450 °C [Fig. 1(a)], indicating that the MgO surface is smooth. The growth of Mn–N is initiated on this smooth MgO(001) surface. Figure 1(b) shows the RHEED patterns obtained following growth, near 25 °C. Similar streaky RHEED patterns are observed from the very beginning of, and throughout, the growth. The primary streaks coincide closely with those of the substrate along both $[100]_{MgO}$ and $[110]_{MgO}$ directions, indicating epitaxial growth. In addition, 1/3 order fractional streaks show up along $[100]_{MgO}$ several minutes after the Mn shutter is opened.

Figure 1(c) shows profiles of MgO and Mn_3N_2 corresponding to the RHEED patterns shown in Figs. 1(a) and 1(b) along the $[100]_{MgO}$ direction. Since the crystal structure of MgO is rocksalt, the atomic row spacing along $[100]_{MgO}$ is $a_{MgO}/2$. Therefore, the spacing between the primary streaks along $[100]_{MgO}$ is $4\pi/a_{MgO}$. A close inspection of the RHEED pattern for Mn_3N_2 clearly shows that the $(-1\ 0)$ and $(1\ 0)$ streaks along every equivalent $[100]_{MgO}$ direction are split into inner and outer streaks, indicating two slightly different atomic row spacings, s_1 and s_2. To determine s_1 and s_2, first we correct the MgO reciprocal lattice spacing for the change due to thermal contraction. We take the lattice constant for MgO at 25 °C to be that found in reference tables, 4.213 Å.[15] Next, we accurately determine the peak splitting by fitting each Mn_3N_2 split peak profile to two overlapping Lorentzian functions, thus obtaining the reciprocal lattice spacing corresponding to s_1 and s_2. Finally, by comparing the two reciprocal lattice spacings for Mn_3N_2 to the reciprocal lattice spacing for MgO (all at 25 °C), we find that $s_1 = 2.103 \pm 0.002$ Å and $s_2 = 2.023 \pm 0.002$ Å. We also note that the spacing between fractional streaks is exactly one-third the spacing of the outer streaks, corresponding to a superlattice with lattice spacing equal to $3s_2$.

We will show that s_1 and s_2 correspond to two types of domains, D1 and D2, where each individual domain has a structure consistent with the fct model of Mn_3N_2 proposed by Kreiner and Jacobs.[8] These two types of domains are equivalent but rotated by 90° with respect to each other. In particular, we find that s_1 and s_2 correspond to the lattice parameters $a/2$ and $c/6$ of the Kreiner model for η Mn_3N_2. Thus, $a = 4.207 \pm 0.004$ Å, and $c = 12.141 \pm 0.012$ Å, with a and c both lying in the surface plane. These values are extremely consistent with the values reported by Kreiner and Jacobs[8] and Suzuki *et al.*[9] for bulk Mn_3N_2.

Shown in Fig. 2 is the Kreiner model for bulk Mn_3N_2. A single unit cell is shown. In this model, every third layer of N atoms is missing. The Mn magnetic moments are aligned along the [100] direction within (001) planes. Moments in successive (001) planes are aligned antiparallel. Not including the spins, we see that the planes of missing N atoms form a superlattice with spacing $c/2$. This agrees with the superlattice spacing measured by RHEED equal to $3s_2$. Thus, the observed superlattice corresponds to the missing third planes of N in the Kreiner model which are normal to the c axis.

NS measurements at room temperature were performed on the BT-9 triple-axis spectrometer at the National Institute of Standards and Technology Center for Neutron Research. The pyrolytic graphite monochromator and analyzer were set to select neutrons with wavelength $\lambda = 2.359$ Å (14.7 meV).

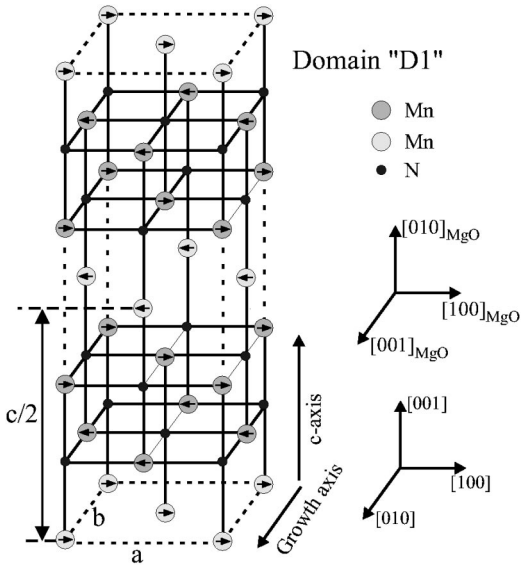

FIG. 2. Model of η Mn_3N_2 for domain D1 is presented. Orientation with respect to the MgO substrate is indicated by two sets of direction vectors. Solid lines indicate the bonds between atoms. Every third (001) plane of N atoms is missing. The arrows in the shaded circles indicate possible orientations of spin.

The sample was oriented with the $[001]_{MgO}$ surface normal and the $[010]_{MgO}$ axes defining the scattering plane (see inset of Fig. 3). Three reflections associated with the η Mn_3N_2 phase are evident in scans along the $[010]_{MgO}$ in-plane direction. The 002 peak at 1.035 ± 0.002 Å^{-1} corresponds to a spacing of 6.071 ± 0.012 Å (three atomic layers), giving a c value of 12.142 ± 0.024 Å. The 004 peak is the second order of 002. The 002, 004, and 006 (only one atomic layer, peak not shown) peaks are structural in nature. The 003 peak at 1.553 ± 0.002 Å^{-1}, which is a magnetic peak originating from the antiferromagnetic alignment of Mn moments in successive planes, corresponds to a spacing of 4.046 ± 0.008 Å (two atomic layers) yielding a c value of 12.138 ± 0.024 Å.

The positions and relative intensities for the 002, 003, 004, and 006 peaks are approximately consistent with those expected from the Kreiner model,[8] thus confirming the existence of the structural domain D1 of η Mn_3N_2 with its c axis parallel to the $[010]_{MgO}$ axis. From our current measurements, we cannot uniquely determine the direction of the Mn moments; however, structure factor calculations suggest that the moments are predominantly confined to the (001) planes.

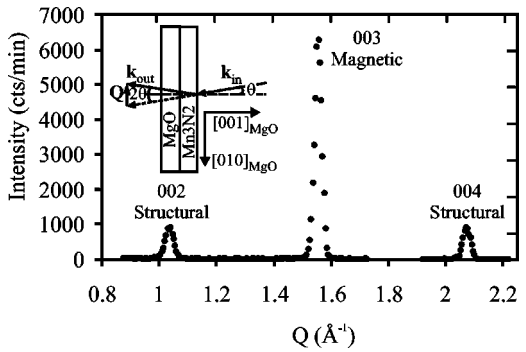

FIG. 3. Neutron diffraction scans parallel to $[010]_{MgO}$ where $Q = 4\pi\sin\theta/\lambda$ are shown. Structural and magnetic peaks from the η Mn_3N_2 phase with the c axis in plane are evident. The inset is a schematic diagram of the neutron scattering geometry. $\mathbf{k}_{in}$ and $\mathbf{k}_{out}$ define the scattering plane. **Q** defines the scan direction.

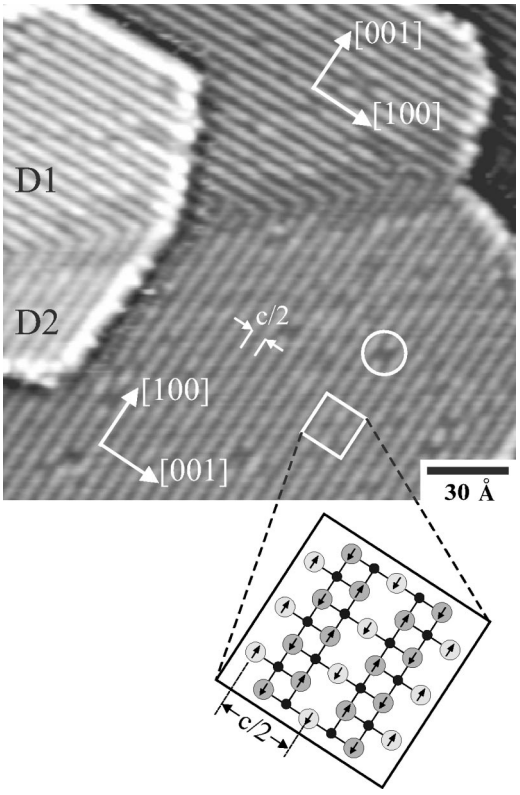

FIG. 4. STM image of η Mn_3N_2 is shown. The image was acquired at a sample bias of -0.4 V and a tunneling current of 0.8 nA. The enhancement at the step edge is due to a local background subtraction. D1 and D2 label two equivalent domains rotated 90° to each other. The white circle marks a point defect. A zoom out shows the corresponding bulk-like model with atoms marked as in Fig. 2.

Based on the fourfold symmetry of the MgO(001) substrate, we also expect to observe the equivalent domain D2, having its *c* axis along $[100]_{MgO}$. Indeed, scans along the $[011]_{MgO}$ axis show a strong antiferromagnetic peak (not shown), indexed as 110. While this 110 peak is not expected from the D1 domain, it is clear evidence for the 90°-rotated D2 domain. Moreover, the existence of this peak shows that the perpendicular lattice parameter of the film is very close to the in-plane *a* value. This is consistent with a fct structure.

Scans parallel to the $[001]_{MgO}$ surface normal also show weak 003_g and 004_g reflections, corresponding to an η Mn_3N_2 domain D3 with *c* axis parallel to the growth (g) direction. The intensity of the 003_g peak is approximately 1/30 of the intensity of the 003 peak shown in Fig. 3. Thus, this orientation is only weakly present in our sample. We conclude that the dominant phase orientation is with the *c* axis in the surface plane for these growth conditions.

Figure 4 shows a 190 Å×190 Å STM image of the η Mn_3N_2 surface obtained *in situ*. Clearly evident are row structures where the spacing between rows is measured to be close to $c/2$.[16] Two domains at 90° to each other are clearly seen in the image (labeled D1 and D2). Two single atomic-height steps are also observed. The row structures cross directly over the steps without interruption or shift, indicating that these surface domains are directly correlated with the bulk domains. The presence of both types of domains, D1 and D2, gives further support to our interpretation of the streak splitting seen in RHEED, as well as to the 110 peak seen in NS.

For comparison with the STM data, we consider the *ac* plane of the bulk model, shown as the zoom out in Fig. 4. We note that the Mn atoms in the missing N planes have only 2 N atom neighbors (on opposite sides). Since these lower coordinated Mn atoms presumably have more dangling bonds, it is likely that they will show a different apparent height compared to the fourfold coordinated Mn atoms in the surface plane. This will thus result in the row structures seen running along [100]. Since the STM image does not distinguish between Mn atoms of a different spin, the periodic spacing of the row structures seen in STM is only $c/2$. The STM image is thus consistent with the symmetry of the bulk truncated model.

Some surface point defects are also observed. One example is circled on the image. These may correspond to single Mn vacancies in the missing N plane.

In conclusion, we have grown Mn_3N_2 on MgO(001) by rf-MBE. We observe smooth, epitaxial growth, as shown by RHEED and STM images. The crystal structure is consistent with a fct model with unit cell given by $a\times a\times c$. Two majority domains D1 and D2, rotated by 90° to each other, both have the *c* axis and one *a* axis in the surface plane. A minority domain D3 is also observed with its *c* axis normal to the surface plane. As seen by STM, the domains D1 and D2 consist of row structures with the rows parallel to [100] for a given domain. Consistent with the result for bulk Mn_3N_2,[8] NS reveals that the Mn moments are aligned in a layered antiferromagnetic arrangement.

The authors gratefully acknowledge help from Florentina Perjeru in coating substrates. This work is supported by the National Science Foundation. One of the authors (H.Q.Y.) also thanks the Ohio University Post-doctoral Fellowship program for support.

[1] J. P. Dismukes, W. M. Yim, and V. S. Ban, J. Cryst. Growth **13**, 365 (1972).
[2] T. D. Moustakas, R. J. Molnar, and J. P. Dismukes, Electrochem. Soc. Proceedings **11**, 197 (1996).
[3] D. Gall, I. Petrov, P. Desjardins, and J. E. Greene, J. Appl. Phys. **86**, 5524 (1999).
[4] D. Gall, I. Petrov, N. Hellgren, L. Hultman, J. E. Sundgren, and J. E. Greene, J. Appl. Phys. **84**, 6034 (1998).
[5] H. A. H. Al-Brithen and A. R. Smith, Appl. Phys. Lett. **77**, 2485 (2000).
[6] A. R. Smith, H. A. H. Al-Brithen, and D. Gall (unpublished).
[7] S. Yang, D. B. Lewis, I. Wadsworth, J. Cawley, J. S. Brooks, and W. D. Munz, Surf. Coat. Technol. **131**, 228 (2000); K. Inumaru, T. Ohara, and S. Yamanaka, Appl. Surf. Sci. **158**, 375 (2000).
[8] G. Kreiner and H. Jacobs, J. Alloys Compd. **183**, 345 (1992).
[9] K. Suzuki, T. Kaneko, H. Yoshida, Y. Obi, H. Fujimori, and H. Morita, J. Alloys Compd. **306**, 66 (2000).
[10] K. Suzuki, H. Morita, T. Kandeko, H. Yoshida, and H. Fujimori, J. Alloys Compd. **201**, 11 (1993).
[11] K. Suzuki, T. Kaneko, H. Yoshida, H. Morita, and H. Fujimori, J. Alloys Compd. **224**, 232 (1995).
[12] T. Dietl, H. Ohno, F. Matsukura, J. Ciberg, and D. Ferrand, Science **287**, 1019 (2000).
[13] H. Ohno, Science **281**, 951 (1998).
[14] Y. Ohno, D. K. Young, B. Beschoten, F. Matsukura, H. Ohno, and D. D. Awschalom, Nature (London) **402**, 790 (1999).
[15] Inorganic Index to Powder Diffraction File (Joint Committee on Powder Diffraction Standards, International Center for Powder Diffraction Data, Swarthmore, PA, 1997): MgO–Card No. 04-0820.
[16] The STM *xy* calibration is approximately known from previous studies of other systems, including ScN(001) and GaN(0001) but not to better than a few percent here.